Solar Energy 150 (2017) 156–160

Contents lists available at ScienceDirect

Solar Energy

journal homepage: www.elsevier.com/locate/solener

Photocurrent enhancement of ultrathin front-textured crystalline silicon solar cells by rear-located periodic silver nanoarrays

Wensheng Yan [a,*], Zhikuo Tao [b], Min Gu [c,d,*], Bryce S. Richards [a,e,*]

[a] Institute of Microstructure Technology (IMT), Karlsruhe Institute of Technology, Karlsruhe 76344, Germany
[b] College of Electronic Science and Engineering, Nanjing University of Posts and Telecommunications, Nanjing 210023, China
[c] Centre for Micro-Photonics, Faculty of Science, Engineering and Technology, Swinburne University of Technology, Hawthorn, Victoria 3122, Australia
[d] Laboratory of Artificial-Intelligence Nanophotonics, School of Science, RMIT University, Melbourne, VIC 3001, Australia
[e] Light Technology Institute (LTI), Karlsruhe Institute of Technology, Engesserstrasse 13, 76131 Karlsruhe, Germany

ARTICLE INFO

Article history:
Received 10 January 2017
Received in revised form 10 April 2017
Accepted 18 April 2017

Keywords:
Photovoltaic
Ultrathin crystalline silicon
Photocurrent enhancement
Silver nanoarrays
Plasmonic effect

ABSTRACT

Ultrathin crystalline silicon solar cells are alternative technology roadmap to achieve more cost-effectiveness. However, when silicon thickness is reduced to less than 50 μm, light absorption loss becomes severe, especially in the long wavelength range of 900–1200 nm. Therefore, it is significant to investigate the enhancements of photocurrent and efficiency by improving light absorption in the long wavelength range. In this work, we design and fabricate approximately 20 μm-thick front-textured monocrystalline silicon solar cells. When periodic silver nanoarrays with precise geometries are applied to the rear of the solar cells, the measured external quantum efficiency clearly reveals an enhancement in the longer wavelengths. For our best sample, the short-circuit current density and the absolute efficiency present the enhancements of ΔJ_{sc} = 0.8 mA/cm^2 and $\Delta\eta$ = 0.6%.

1. Introduction

Over the past few decades, crystalline silicon (c-Si) solar cells have dominated the global photovoltaic market (www.itrpv.net, 2015). Although the module cost has been remarkably reduced in the past tens of years, the present cost is still high compared with fossil-fuel based energy. At present, commercial c-Si solar cells are typically 180 μm in thickness. But, the cost of the silicon material alone accounts for up to ~40% of total module cost (www.itrpv.net, 2015). Therefore, developing ultrathin c-Si solar cells is potentially alternative technology roadmap with the benefit of more cost-effectiveness. However, it is noted that experimental reports about fabrications of ultrathin c-Si solar cells still rare till now. In addition, these reports are mainly based on single-sided, front-textured crystalline silicon (Petermann et al., 2012; Jeong et al., 2013; Wang et al., 2014; Branham et al., 2015), which is relevant with silicon thickness and the present state of the art. On the other hand, when the thickness of crystalline silicon wafers is reduced to less than 50 μm, light absorption loss becomes severe, especially for the long wavelength range of 900–1200 nm. As a result, effective addressing of the light absorption loss in this longer wavelength range is significant for developing highly efficient ultrathin c-Si for photovoltaics.

Keeping the above key questions in mind, in this work, we design and fabricate approximately 20 μm-thick, front-textured monocrystalline silicon solar cells. To improve light absorption in longer wavelengths above 900 nm, hexagonal arrays of periodic silver nanoparticles with precise geometries are applied and integrated on the rear of solar cells via nanoimprinting lithography (NIL). Via plasmonic light-trapping effect, the rear-located silver nanoarrays are adopted because this design of rear-location can avoid detrimental Fano effect in short wavelengths, which usually occurs for the case of solar cells with front-located silver nanoparticles due to the interference effects between the incident and scattered light (Beck et al., 2009; Lassiter et al., 2010; Yang et al., 2012; Green and Pillai, 2012; Atwater and Polman, 2010; Catchpole and Polman, 2008a,b; Pillai et al., 2007; Yan et al., 2013; Mokkapati et al., 2009). In addition, compared with disordered silver nanoparticles (Yang et al., 2012; Beck et al., 2010), the nanoimprinting technique with the fabrication capability of ordered silver nanoarrays is of not only high reproducibility but also offering a unique capability to precisely control the geometry of each nanoparticle

* Corresponding authors at: Institute of Microstructure Technology (IMT), Karlsruhe Institute of Technology, Karlsruhe 76344, Germany (W. Yan); Centre for Micro-Photonics, Faculty of Science, Engineering and Technology, Swinburne University of Technology, Hawthorn, Victoria 3122, Australia (M. Gu). Institute of Microstructure Technology (IMT), Karlsruhe Institute of Technology, Karlsruhe 76344, Germany (B.S. Richards).

E-mail addresses: wensheng.yan@kit.edu (W. Yan), min.gu@rmit.edu.au (M. Gu), bryce.richards@kit.edu (B.S. Richards).

http://dx.doi.org/10.1016/j.solener.2017.04.046
0038-092X/

as well as the pitch of the arrays (Guo, 2007; Battaglia et al., 2011). In principle, precise manipulation of each nanoparticle physically offers a potential to maximize the light absorption by precisely tailoring the optical scattering properties of nanoparticles with excellent experimental repeatability.

2. Design and fabrication

Geometry parameters of rear-located periodic silver nanoarrays are designed and optimized by using the finite-difference time-domain (FDTD) commercial software (www.lumerical.com). Periodic silver nanoarrays with a hexagonal distribution are adopted in this work. During the present simulation, complex dielectric functions (n, k) of Al_2O_3, Al, and SiO_2 are taken from Palik (1998) whereas the optical constants of Ag, crystalline Si and SiN_x are from Johnson and Christy (1972), Green (2008), and Kim et al. (2014), respectively. The optimal geometry parameters of each silver nanoparticle are approximately the height of 100 nm and the diameter of 180 nm in a hemisphere-like shape as well as the pitch of about 400 nm.

Fig. 1 shows cross-sectional schematic of single-sided front-textured monocrystalline silicon cell architecture, where silver nanoarrays are located at the rear of the cell. As shown in Fig. 1, Al_2O_3/SiN_x on the front surface plays the roles of anti-reflection as well as passivation. Here the Al_2O_3 thin film thickness is 3 nm and SiN_x thin film is used with a standard thickness. In the present work, SiN_x and Al_2O_3 thin films are prepared by plasma enhanced chemical vapour deposition (PECVD) and atom layer deposition (ALD), respectively.

In this work, we use *p*-type c-Si wafers with phosphorus-doped emitters. The typical passivated emitter and rear cell (PERC) structures are prepared, where the front contact is Ni/Cu and back contact is Al. Regarding the fabrication procedure of the rear of solar cells shown in Fig. 1, a SiO_2 dielectric spacer with 18 nm is deposited on the rear of silicon wafer via PECVD with the purpose to increase optical scattering cross section of silver nanoarrays via plasmonic effect. Then, periodic silver nanoarrays are imprinted on the spacer layer via the NIL (NX-B200). Following this, another thick SiO_2 layer is deposited on silver nanoarrays to form the embedded silver nanoarrays in SiO_2 layer. We present a flow chart to show how we prepare the samples as shown in Fig. 2, where a thick silicon wafer is initially used. A scanning electron microscope (SEM) image of silicon surface texture with random small pyramids is shown in Fig. 3, where small pyramids are beneficial to both preparations and performance of ultrathin silicon solar cells compared with large pyramids with the range of 3–10 μm by conventional industry procedure.

Three-step fabrication flowchart for silver nanoarrays via the NIL is shown in Fig. 4, where the array is hexagonal. Step 1 is a mould preparation via electron beam lithography (EBL) as shown in Fig. 4(a), respectively. The area of single mould is 10 mm^2 in a square. Step 2 is a patterning fabrication via the NIL on the substrate. A SEM image is shown in Fig. 4(b). When the imprinting process is finished, a reactive-ion etching (RIE) is used to remove residual resist inside holes. Step 3 is a silver thin film deposition by electron-beam evaporation. After that, the photoresist can be removed by a chemical solution and periodic silver nanoarrays with hexagonal arrangement are obtained as shown in Fig. 4(c). The right-bottom inset of Fig. 4(c) shows a photo of the fabricated solar cell with approximately 1 cm^2 showing the NIL capability.

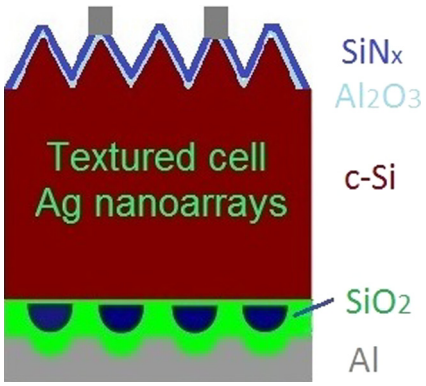

Fig. 1. Cross-sectional schematic of front textured monocrystalline silicon solar cell architecture.

3. Results and discussion

The measured wavelength dependent external quantum efficiencies (EQEs) of the planar cell and the textured cells with and without rear-located silver nanoarrays over the whole wavelength range of 300–1200 nm are shown in Fig. 5(a). The details of the planar cell refer to the supplementary Information. The reflectance of these solar cells are measured and thereby the absorption of the three cells are obtained and plotted in Fig. 5(a) based on the relationship A = 1 − R, where A is absorption and R is reflectance. Compared with the planar solar cell, it is seen in Fig. 5(a) that the EQE is significantly improved in the whole wavelength range of 300–1200 nm for the textured silicon solar cell, which is mainly attributed to that the front pyramidal texture increases the total light propagation path and thus improves light absorption in crystalline silicon. Compared with the textured cell without silver nanoarrays, the rear-located silver nanoarrays significantly improve the EQE and absorption in longer wavelengths starting from near 900 nm. The internal quantum efficiency (IQE) is calculated by using the relationship IQE = EQE/(1 − R) and shown in Fig. 5(b). It is seen in Fig. 5(b) that compared with the textured cell without silver nanoarrays, the IQE also reveals an enhancement in the long wavelength range for the textured cell with silver nanoarrays. This IQE improvement is attributed to the silver nanoarrays induced plasmonic effect resulting in the light absorption enhancement in longer wavelengths.

If everything is ideal for the two devices, the IQE of the planar device should be higher than the IQE of textured silicon device (without rear silver nanoarrays) at short wavelengths. This is due to the front textured surface possessing a larger front surface area and, thus, higher surface recombination velocity. At the same time, the IQE of the planar device should be similar to the IQE of the front textured silicon device at long wavelengths, since the rear surfaces of both devices are planar. However, for a real device, the surface recombination velocities depend not only on the surface area but also on other factors, including the chemical surface treatment quality or residual ionic contamination. It is seen from Fig. 5(b) that the IQE of the planar device is lower than that of either of the textured silicon devices over the entire wavelength range. The most likely reason for this is the higher residual ionic contamination on the surfaces or poor surface treatment quality leads. Both of the factors could contribute to higher surface recombination velocities for the planar device compared with the front textured device. This is based on the fact that the textured silicon devices experiences two chemical surface treatments – before and after texture, respectively – while the planar silicon experiences one chemical surface treatment. In fact, the effects of surface treatment quality or residual ionic contamination on photovoltaic devices have also been observed in the literature (Buchholz, 2016; Kim et al., 2017).

To further investigate the optical path enhancement between the textured silicon cells with and without silver nanoarrays, the IQE analysis method is employed in this work (Rand and Basore,